Miscellaneous Studies of ^{16}N Data

X.Chen
Lawrence Berkeley National Laboratory
SNO-STR-99-018

November 23, 1999

Abstract

The standard SNOMAN time fitter has been studied and found to mis-reconstruct many ^{16}N events. Possible causes of mis-reconstructions have been studied. A new vertex fitter, reported here, was developed to improve both event reconstruction accuracy (event position) and the determination of the recoil electron direction (event direction). Anisotropy measurements of ^{16}N events from both the decay chamber and the umbilical cord are presented. The differing nature of chamber and umbilical cord events and the agreement between ^{16}N data and Monte Carlo simulations support the value of the θ_{ij} parameter in evaluating the multiplicity of events in the SNO detector.

1 Introduction

^{16}N source is the first energy calibration source used in the detector. This source provides us important data to 1) evaluate our event reconstruction tools 2) obtain an energy calibration for charged current events 3)provides us an important test bed to "calibrate" other event characterization tools and 4) to further refine our Monte Carlo simulations of the SNO detector and detector response.

Data from run3597 (19990520) was used on the following analyses. LBL's ^{16}N decay chamber was nominally located at the position (-16.03, 23.50, -0.1). ^{16}N events were selected by setting a threshold on Q_{lx} of the small PMT located inside the chamber. ECA/PCA calibration constants produced by B.Frati were used in the studies.

2 The vertex fitter

A vertex fitter is an essential tool in any SNO data analysis. The determination of the event location and direction are critical in obtaining a correct energy determination and insetimating the detector efficiency. There are four different vertex fitters in SNOMAN, among which the time fitter is the quickest and the most often used one. Thus it is important that the performance of such fitter is checked against the real data.

Normally the performance of a vertex fitter is judged according to two criteria (see figure 1):

1. Peak position and width of the Rdev distribution. This describes accuracy of the fitter for majority of events.

2. The ratio of peak to tail of events in the Rdev distribution. For experiments, such as SNO, with a low signal to noise ratio, events with significant reconstruction errors impose a significant limitation to the experiment.

The extremely large number of background events near the PMTs and in the light water makes the second criterion is more critical for SNO. We require good event reconstruction to better define true physics events within our fidual volume and to minimize the accidental inclusion of background events within the same volume. To a lesser degree the efficiency of the fitter in keeping true CC events should also be considered, but this must also be well characterized. It is difficult to use the ^{16}N source to evaluate the first criterion. The light creation process (Compton scattering of the source=92s gamma rays) results in light being created in a large volume around the 16N chamber. A volume much larger than SNO intrinsic resolution of 10 cm.

The following method has been used (e.g. [1]) to check the performance of the fitter with ^{16}N data against the second criterion. First events are selected that arereconstruct a significant distance away from the chamber (*1.5 m). Second a θ parameter is calculated for each event following the geometry presented in figure 2. The reconstructed distance between the event source (16N chamber) and the event source (Compton scattering site) is selected to be large enough to result in angular parameter, θ, that can distinguish between well and poorly reconstructed events. That is, if the fitter correctly reconstructs an event vertex then the calculated θ parameter should be small indicating the alignment of the outward going gamma ray with the resulting recoil electron. We illustrate the imposition of the radial cut also reduces the effects of the decay chamber, primarily shadowing of backwards traveling light.

Results of the time fitter are presented in figure 3. There are two peaks clearly visible; the one anticipated near $\theta \approx 0^o$ and a second peak near $\theta \approx 180^o$. These events in the backward peak, we deem to be poorly reconstructed events. We impose a 150-cm radial cut, accepting only those events outside this distance from the ^{16}N chamber. Therefore, either the fitted vertex or the fitted direction (or both) must be incorrect to form the peak at $\theta \approx 0^o$. The fitted direction in the time fitter is just the average photon direction. Therefore, we conclude the fitted vertex is more likely to be the origin of these events. We can test this hypothesis using additional information event information obtained from the 16N source. This source is a triggered source, defining each event=92s PMT hits to the beta trigger in the source. However, before using this "absolute" timing information it is important to recognize that longer than anticipated umbilical cord results in the detector frequently triggered due to PMT signals before the external trigger input can trigger the detector. It is important to adjust the PMT time to the time of the scintillator signal if we wish to use the "absolute" time in comparing events. After performing this time correction, an interesting feature in the fitted time distribution for ^{16}N events is observed when graphed against the calculated distance between the ^{16}N decay chamber and the fitted event vertex. This feature is presented in figure 4. We observe two bands of events in the plot. The positive slope band is anticipated

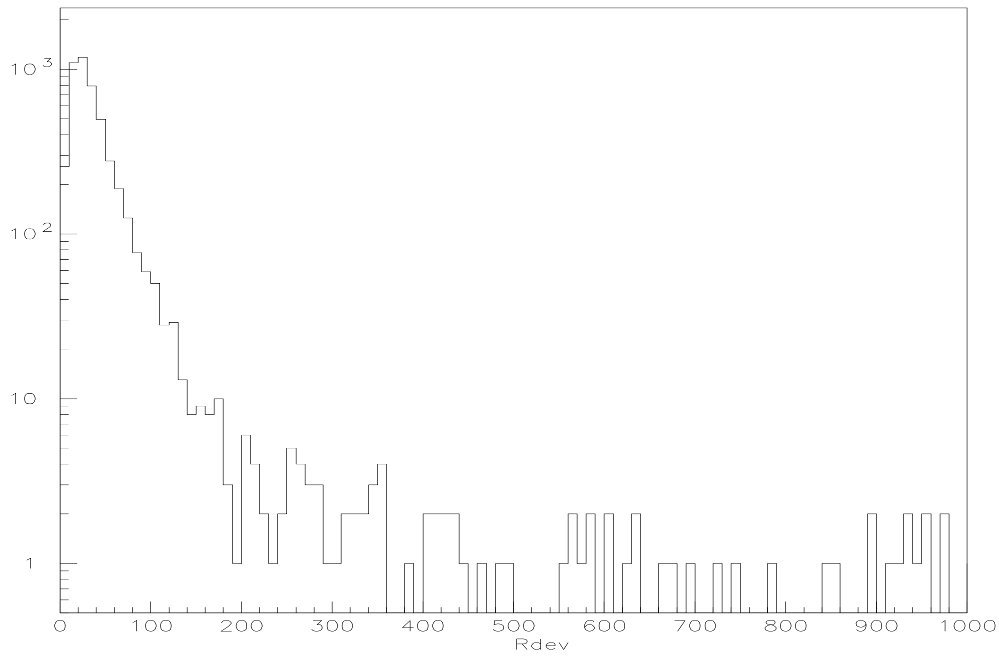

Figure 1: Rdev (distance between the actual vertex and the fit vertex) distribution of the time fitter on charged current events.

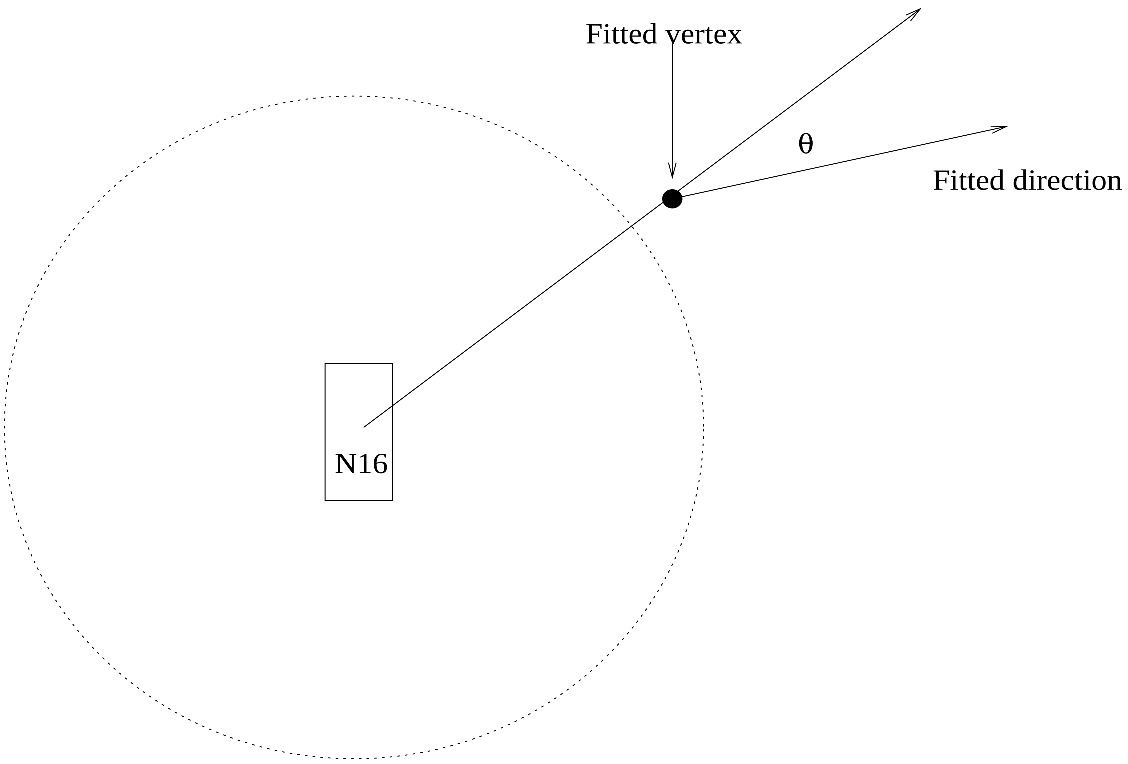

Figure 2: Definition of θ used in evaluation of fitter performance on the ^{16}N data.

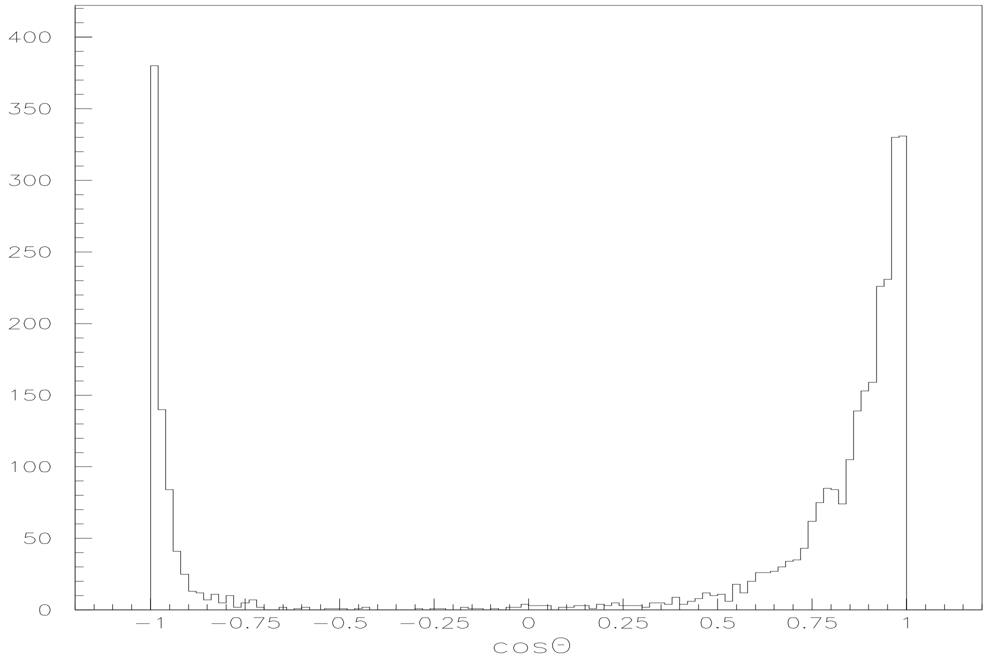

Figure 3: $cos\theta$ distribution of $16N$ events fitted with the time fitter. Only events reconstructed between 150 cm and 600 cm away from the source are included in the plot.

and the slope of this band yields the speed of light in water with the later times corresponding to the time for the outgoing gamma ray to travel further before converting in the water.. The negative slope band, we conclude, results from poor event vertex reconstruction. It is interesting that the absolute value of this band is very close to the slope of the anticipated band. Most of the events in the negative slope band converted fairly close to the source and many of the backward going photons could be absorbed or scattered by the source canister. This absorption results in a significant reconstruction error. As a consequent the events are reconstructed on the wrong side of= the source. Events would then appear to occur earlier than the light detected in the plastic scintillator. We confirmed this hypotheses by placing a cut on the fitted time (time ¿280 ns) to effectively remove the negative slope band. The resulting angular distribution, shown in figure 5, illustrates that the time cut eliminates the peak at $\theta \approx 0^o$ while retaining most of the forward peak. Furthermore, SNOMAN simulations reproduce the two bands of events shown in figure 4, see [1].

The 16N data clearly shows the time fitter needs to be improved. We can not impose a similar cut on fitted time for neutrino events, lacking a definition of absolute time for these events. What has been shown is that for events where backward going light is blocked or scattered there is significant fitter push. We don't know for sure the same effect applies for neutrino events where there is no large object blocking the light. We developed a new vertex fitter to assist in fitting simple (low multiplicity) events. Like the time fitter, this fitter determines the fitted vertex and direction by

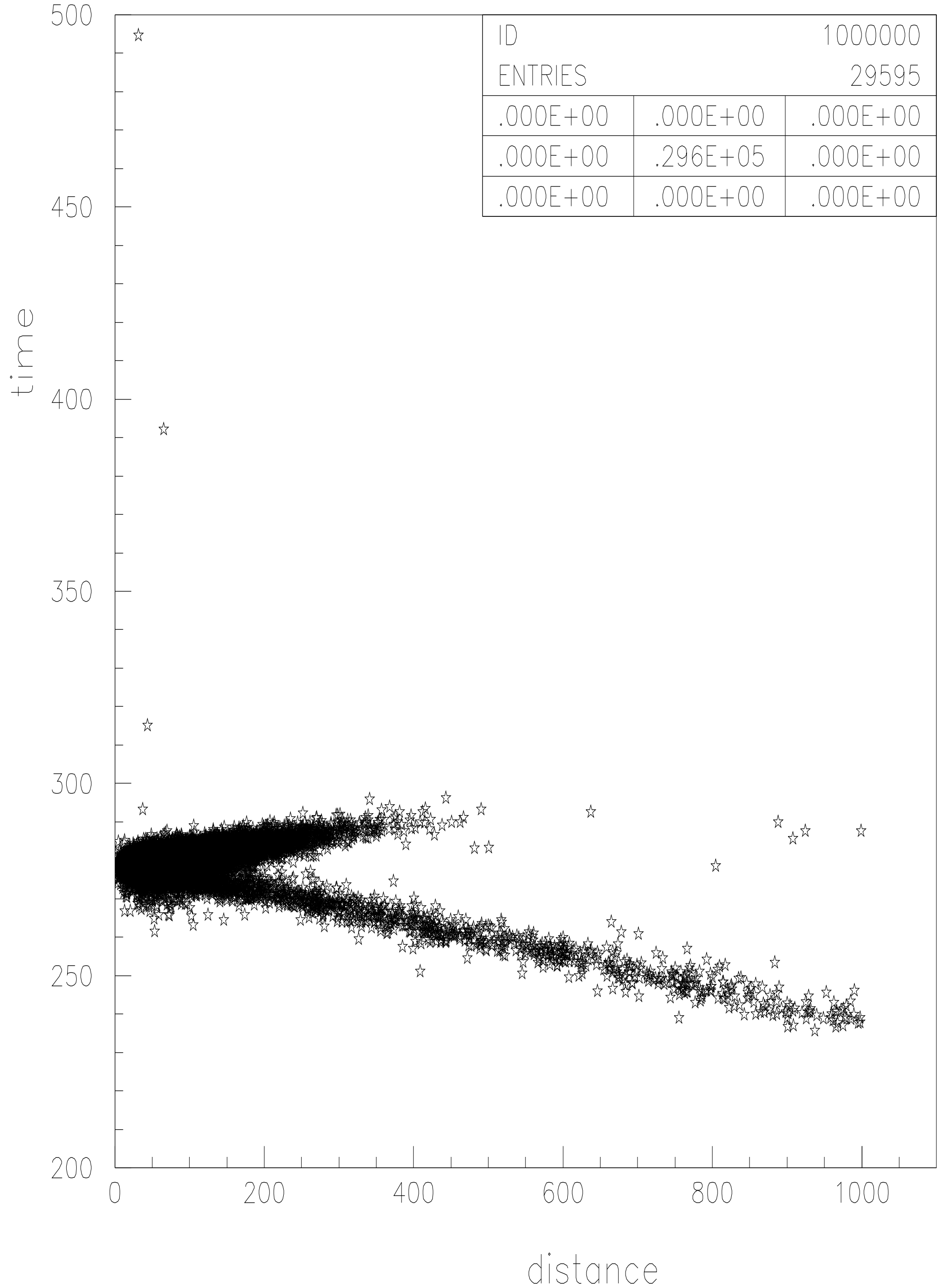

Figure 4: Distance (between the fitted vertex and the source) vs. the fitted time. The fitted time has been corrected with the source trigger information (see text). The time fitter was used and events were restricted within 10 meters of the source

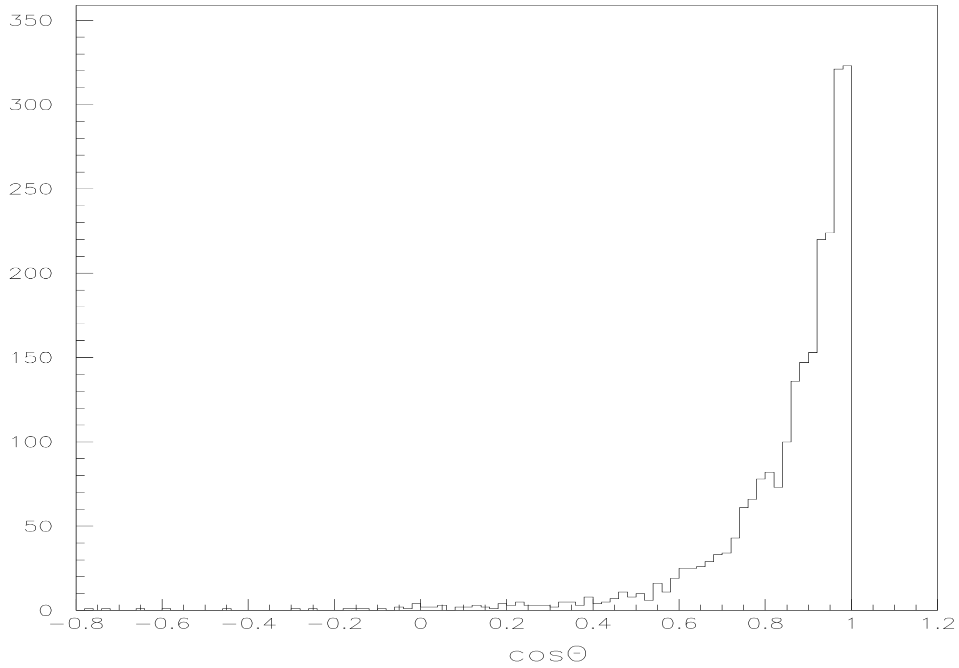

Figure 5: $cos\theta$ distribution of $*16N$ events fitted with the time fitter. A cut on the fitted time (time > 280ns) was imposed. Only events reconstructed between 150 cm and 600 cm away from the source are included in the plot. The time fitter was used.

minimizing the following χ^2 function:

$$\begin{array}{c} \chi^2 = \chi_1^2 + \alpha \times \chi_2^2 \\ \chi_1^2 = \sum_i (\frac{\triangle t_i}{\sigma_t})^2 \quad \triangle t_i = MIN(\left| t_i - t_{fit} - \frac{d}{v_c} \right|, 3\sigma_t) \\ d = \sqrt{(x_i - x_{fit})^2 + (y_i - y_{fit})^2 + (z_i - z_{fit})^2} \\ \chi_2^2 = \sum_i (\frac{\triangle \theta_i}{\sigma_\theta})^2 \quad \triangle \theta_i = MIN(|\theta_i - \theta_c|, 3\sigma_\theta) \end{array} \tag{1}$$

where t_i, x_i, y_i and z_i are the temporal and spatial coordinates of the i^{th} PMT hit; t_{fit}, x_{fit}, y_{fit} and z_{fit} are the temporal and spatial coordinates of fitted vertex; σ_t is width of the PMT transit time (1.7ns), θ_c is the Cerenkov angle (42^o); θ_i is the angle between the event fitted direction and direction of the i^{th} hit; σ_θ is roughly width of the angular distribution of Cerenkov light (8^o) and v_c is speed of light in water (22.396cm/ns). Compared with the χ^2 function used in the time fitter, a couple of things are worth mentioning regarding to this χ^2 function:

- Both time and angular information are included. They are weighted by a factor α which can be tuned by the calibration data. Thus this fitter have 6 parameters to fit: 4 coordinates of the vertex and 2 angles of the direction.

- Instead of using full Gaussian function as underlying probability distribution function, the new fitter uses the so called truncated Gaussian function.

In addition, several technique are used in the fitter:

- Before the actual fitting, a time window (76ns which is roughly how long it takes for a photon to fly from one end of the detector to the other) is slid through the time of all PMT hits to determine a cluster of hits which maximizes number of hits falling in the window. Only hits falling inside the "maximized" window are used in the later fitting and center of the window is used as the initial value for t_{fit}.

- Because derivative of the new χ^2 function is not calculable, the down hill simplex method adapted from [2] was used to minimize the χ^2 function. If during the minimization, the vertex position is pushed more than 10 meters away from center of the detector, the χ^2 value will be set as 1e10 so that the next minimization step can push the current vertex back inside the detector.

- Similar to the time fitter, an iteration is carried out to throw away the bad hits continuously until all of the remaining hits fall inside a pre-defined time window. This time window is also chosen to be asymmetric around the main event peak to preferentially reject the more often late hits.

- After the algorithm converges and the fitted vertex is fixed, a grid search is carried out in (θ, ϕ) space to minimize the χ_2^2 function stated in equation 1 in order to fit the direction separately.

Performance of the fitter is shown in figure 6. The event band with the negative slope is almost gone while the event band with the positive slope is more or less retained. Efficiency of the new fitter is almost the same as that of the time fitter. Figure 7 shows the corresponding $cos\theta$ distribution. Without any time cut, the backward peak is almost gone. In the author's opinion, judged by the second criterion stated above, this is a very strong evidence that the new fitter is much better than the time fitter. Improvement on performance of the fitter can be due to several factors:

- The sliding window helps to reject bad hits. However, as both the time fitter and this new fitter use iteration to throw out bad hits, the effect should be fairly small.

- Inclusion of the angular information in the χ^2 function certainly help reducing the so called fitter pull effect. Because time information is much more robust and accurate than the angular information, χ_1^2 and χ_2^2 have to be weighted. From author's experience, the angular information does not appear to help much in reconstructing event vertex, although it certainly is very useful in fitting event direction.

- In the author's opinion, the most important element in this fitter is that it uses a truncated Gaussian rather than a full Gaussian as the p.d.f.. Certainly by such way, the fitter is much more robust against bad hits which no longer have much larger weights than good ones in the χ^2 function described in equation 1.

This new fitter has to be checked against the first criterion stated above. As we don't have any point source, some charged current events generated by Monte Carlo have been used to compare two fitters. As shown in figure 8, peak positions of 2 Rdev distributions are more or less the same. The new fitter works much better in

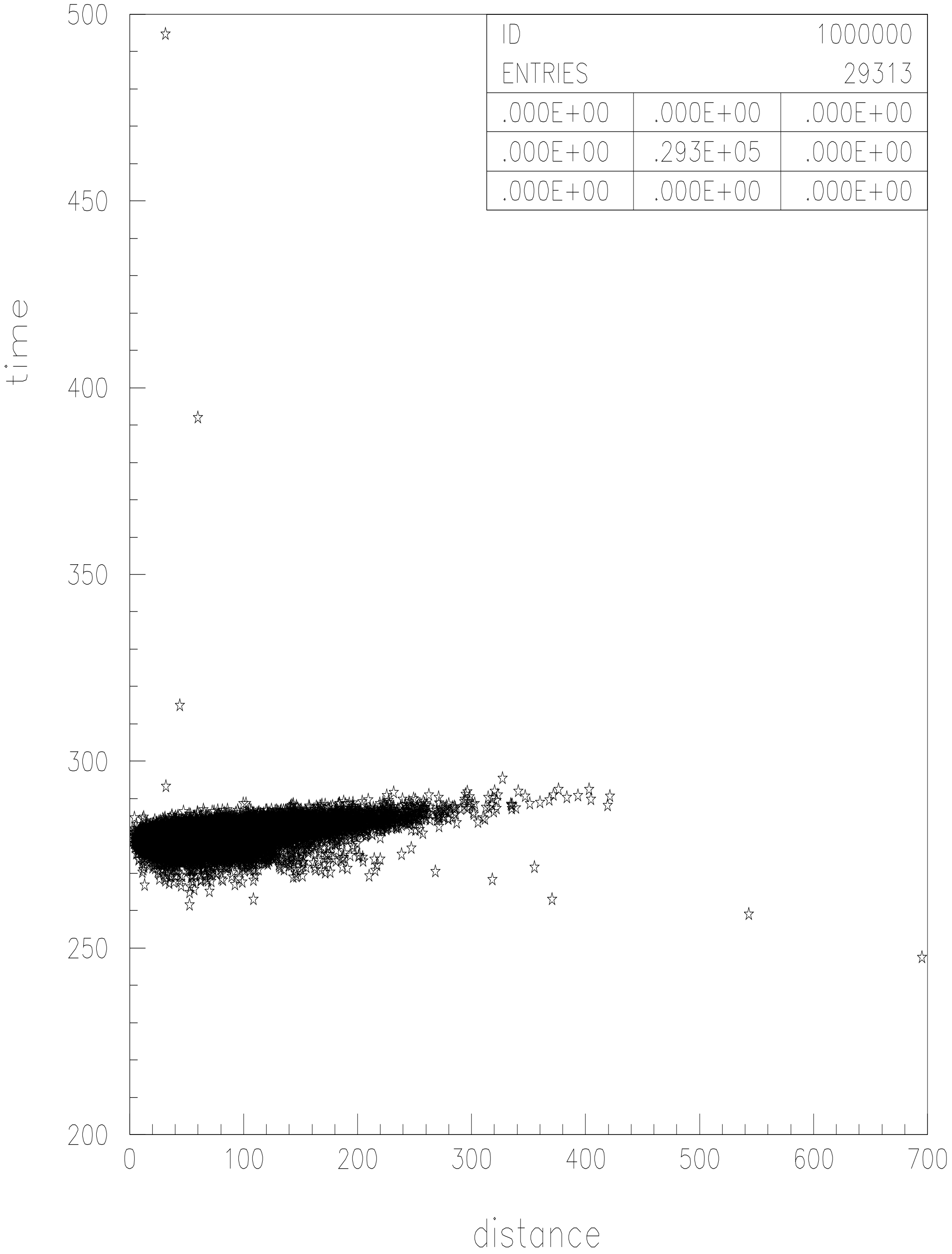

Figure 6: Distance (between the fitted vertex and the source) vs. the fitted time, cut on distance < 1000cm, the new fitter was used

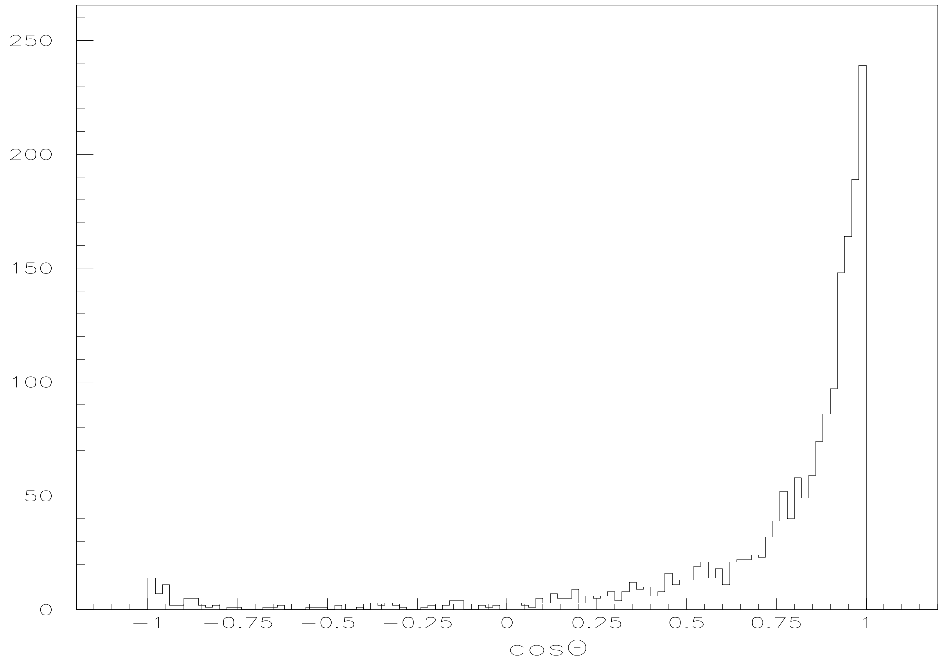

Figure 7: $cos\theta$ distribution of $*16N$ events fitted with the time fitter. A cut on the fitted time (time $>$ 280ns) was imposed. Only events reconstructed between 150 cm and 600 cm away from the source are included in the plot.

reconstructing event direction, as shown in figure 9. This is not surprising as the fitted direction in the time fitter is just the averaged direction of all hits, it does not use the fact that many of the photons are emitted along the Cerenkov cone.

Surely the actual time p.d.f. for SNO events is neither Gaussian nor truncated Gaussian, while we may never know what is the true p.d.f., usage of a truncated Gaussian in the fitter certainly improves the fitter performance and it has been proved with real data. Inclusion of the angular information in the vertex reconstruction may help to reduce the fitter pull. However, it seems tricky to do this and it is certainly inappropriate to fit a multiple particle event such as a NC event with the assumption that it tends to produce light along the Cerenkov cone. On the other hand, inclusion of the angular information certainly help reconstructing event direction, it should be used in future analyses of CC data. There are many other ways by which performance of the fitter could be improved such as using better minimizing algorithm and maximum likelihood method. It will be much better if we can have a electron source to test different fitters.

3 Anisotropy of light from ^{16}N Events

To begin our examination of 16N events using the new vertex fitter, we present the θ and ϕ distributions in figure 10. The dip at $cos\theta \approx 0.75$ from the anticipated flat distribution is not understood at this time.

A more interesting approach is to look at the θ_{ij} distribution from the calibration

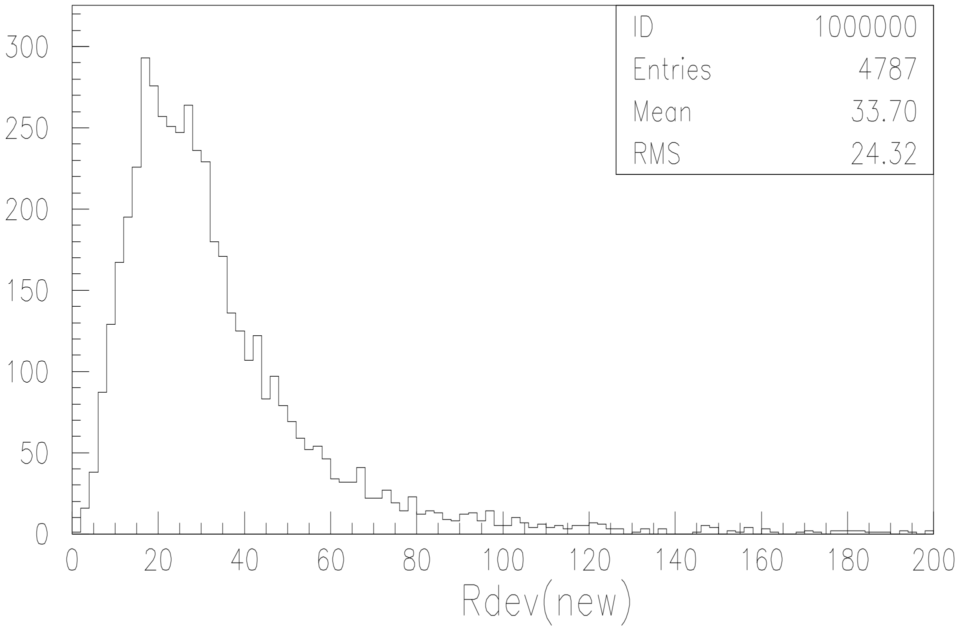

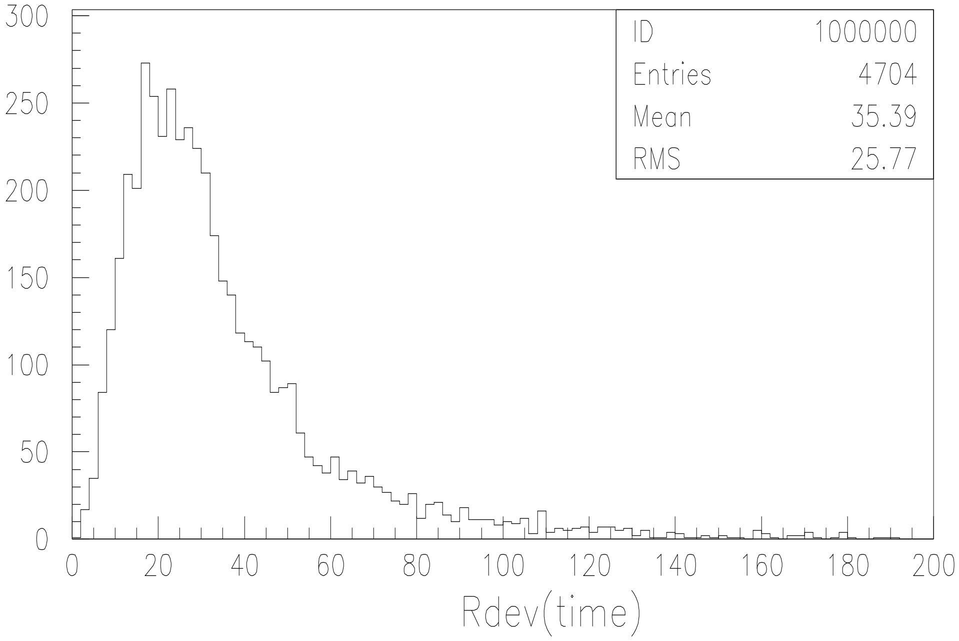

Figure 8: Rdev (distance between event fitted vertex and its actual vertex) distributions for 5000 CC events: upper plot (new fitter), lower plot (time fitter), cut on Rdev $<$ 200cm.

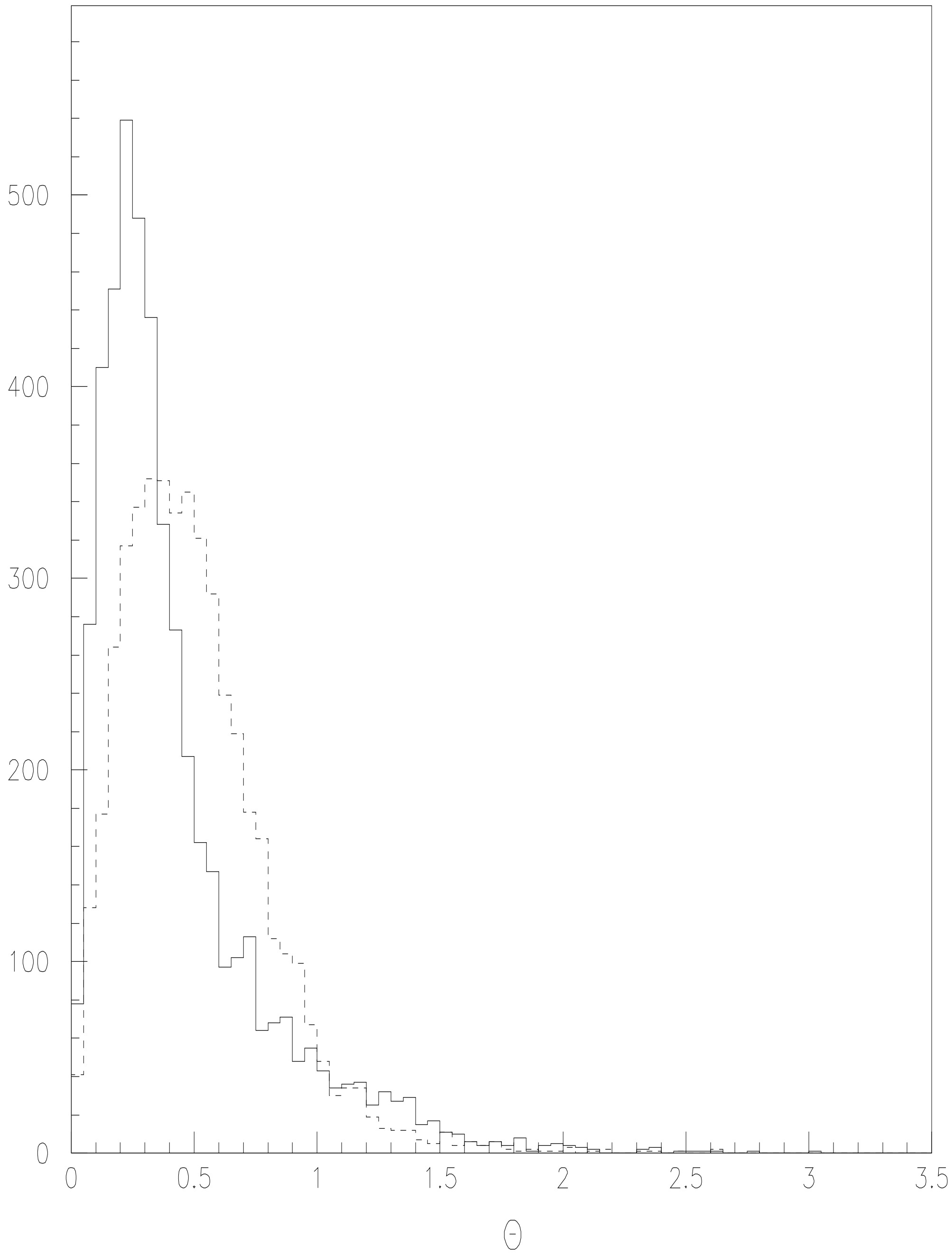

Figure 9: Angle between the event fitted direction and its actual direction, solid line(the new fitter), dashed line(the time fitter).

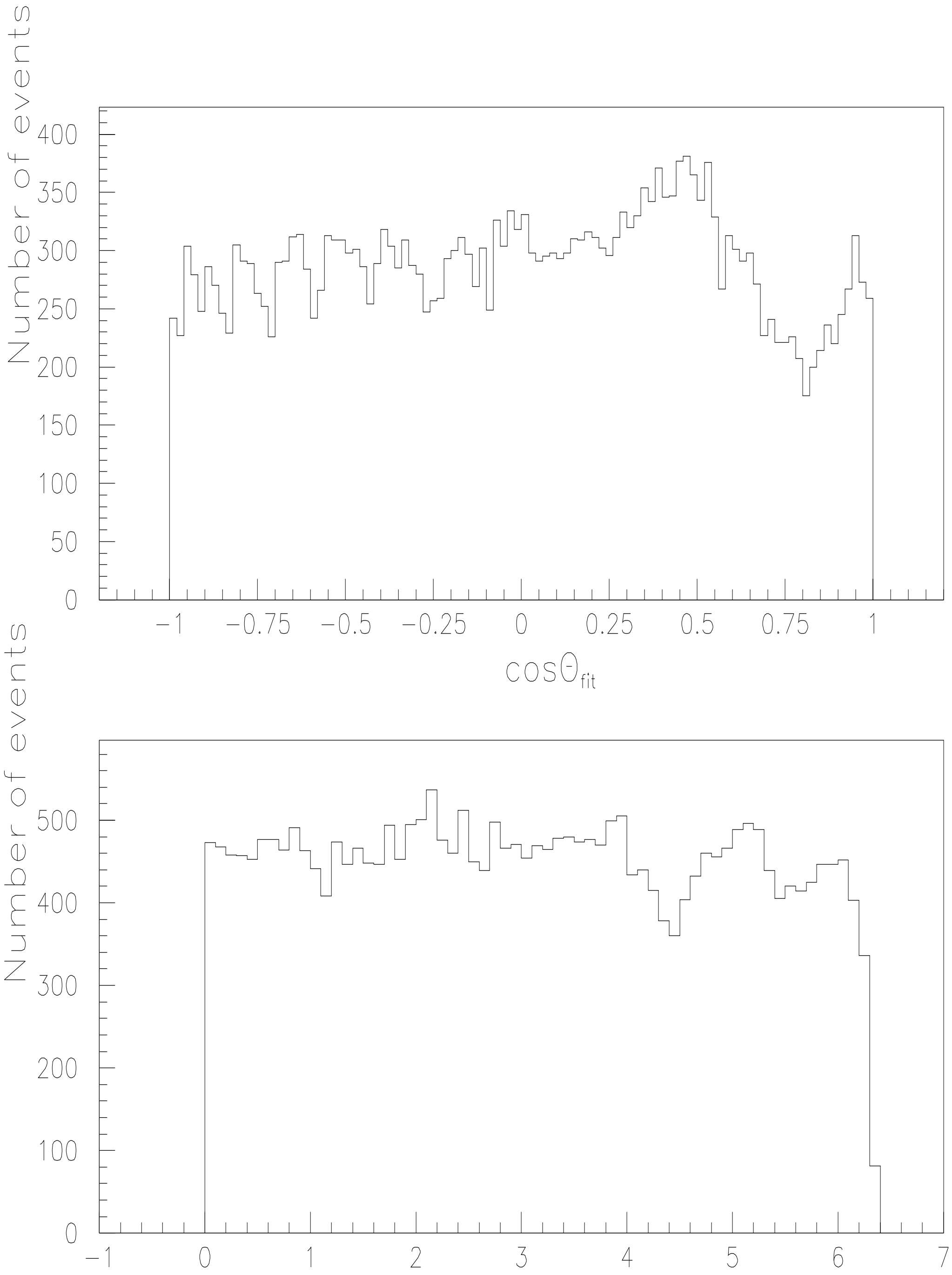

Figure 10: $cos\theta$ and ϕ distributions of the ${}^{16}N$ events using new fitter.

source. As umbilic cord of the ^{16}N source is made of acrylic, some electrons can escape from the umbilic and produce light in the detector. 26% of ^{16}N decays produce a single 10.4Mev electron while 68% of decays produce a 4.3Mev electron and a 6.1Mev gamma. Because most of energy carried by the electron will be absorbed by the umbilic, majority of light produced by an umbilic event come from the gamma. During the following data analysis, the ^{16}N events (from the decay chamber) are defined as the events with a scintillator signal and reconstructed within 2 meters of the decay chamber while the umbilic events are the events without the scintillator signal and reconstructed within a cylinder of the umbilic ($0 \leq \sqrt{x_{fit}^2 + y_{fit}^2} \leq 200cm$ and $200cm \leq z_{fit} \leq 400cm$). As figure 11 shows, Nhits distribution of the umbilic events has a larger mean value than that of the events from decay chamber which indicates some of escaping electrons really contribute to total light output of the umbilic events. Figure 12 shows the θ_{ij} distribution from the ^{16}N events produced by the data and Monte Carlo (upper plot) and the corresponding distributions for the umbilic events (bottom plot). Definition of the θ_{ij} parameter can be found in [3]. Basically, it is a parameter which measures isotropy of light produced by a event. More isotropic the angular distribution, larger the θ_{ij} value. Both sets of distributions were produced with a nhits cut $nhits \geq 40$. Because many of the umbilic events are two-particle events, it is expected that on average a umbilic event has a larger θ_{ij} than a ^{16}N event. This is clearly shown in the figure, the real data and the MC data agree with each other fairly well for both types of events. In the author's personal view, this is a clear evidence that the SNO detector is able to see statistically the angular difference between a single particle event and a multiple particle event at such energy level. As during a single run the umbilic events and the ^{16}N events come from different positions inside the detector, a more fair comparison should be made between the data from a run where the ^{16}N source was deployed at the center of the detector and the data from a run where the source was deployed well below the center. Figure 13 presents two θ_{ij} distributions for the umbilic events with the source located at different positions. Two distributions agree with each other well. This is a evidence that the θ_{ij} parameter is relatively independent of the source position, it is also less sensitive to the energy scale of the detector as run4514 was after magnetic coil was turned on and there was roughly 10% increase of nhits with the magnetic coil on.

4 Conclusion and Comments

We have presented a new vertex fitter and analyzed it performance using the ^{16}N data. Significant enhancements in event reconstruction for simple events are demonstrated with ^{16}N data and Monte Carlo simulations. Performance of the fitter could be further enhanced by applying a global search (similar as the technique used in the grid fitter) to avoid local minima. An electron source would be very valuable for studying fitter performance as mean path of an electron is much less than resolution of the detector.

Using the difference is light anisotropy from umbilical cord events and ^{16}N chamber events, we have demonstrated the efficacy of the θ_{ij} parameter in distinguishing simple (single particle) from complex (multiparticle events at higher energies (6

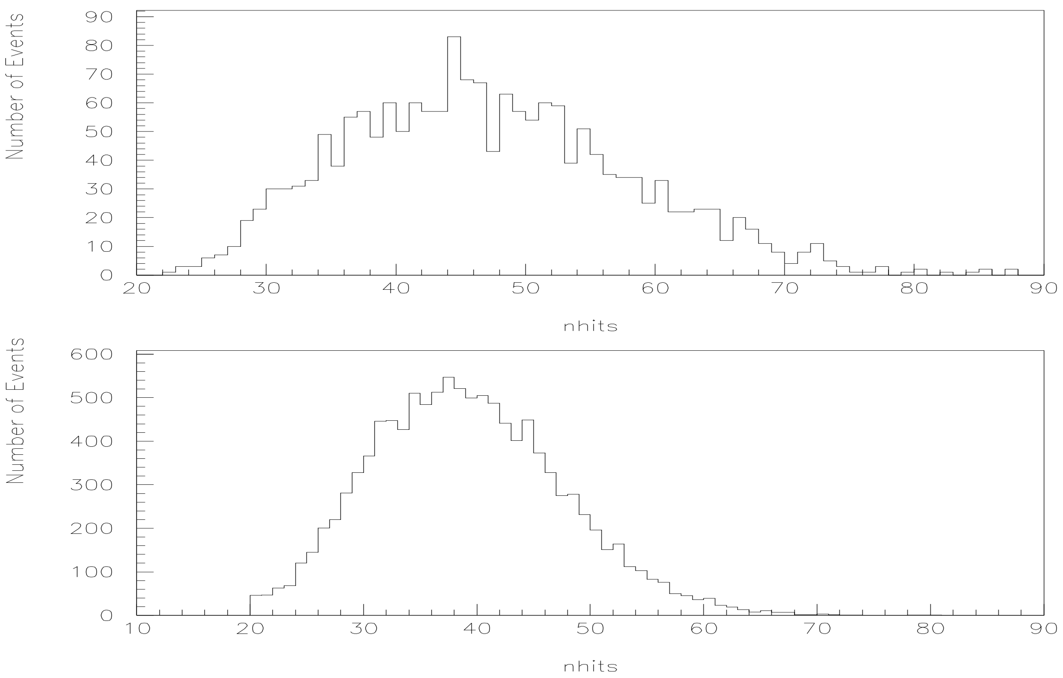

Figure 11: Nhits distributions for the ^{16}N events (bottom plot) and the umbilic events (upper plot).

MeV) on a statistical basis.

References

[1] C.J.Jillings, The Electron-Scattering Reaction in the Sudbury Neutrino Observatory, Ph.D thesis, Queen's University, Canada.

[2] W.H.Press, S.A.Teukolsy, W.T.Vettering and B.P.Fiannery, Numerical Recipes, Cambridge University Press, 1992.

[3] Xin Chen, Monte Carlo Simulations and Analyses of Backgrounds in the Sudbury Neutrino Observatory, August 1998, DPhil thesis, the Oxford university.

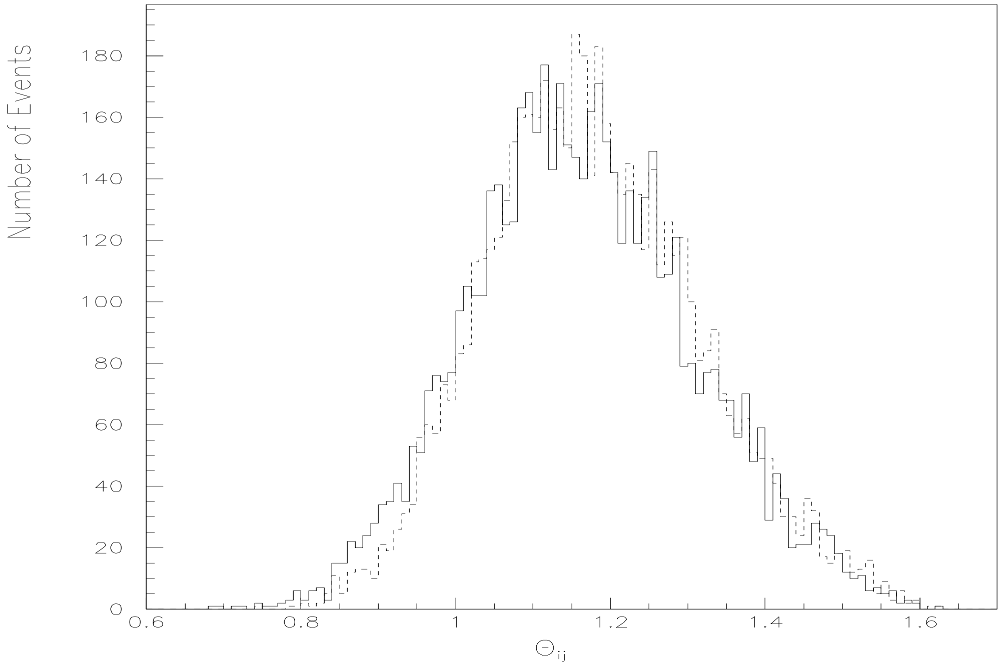

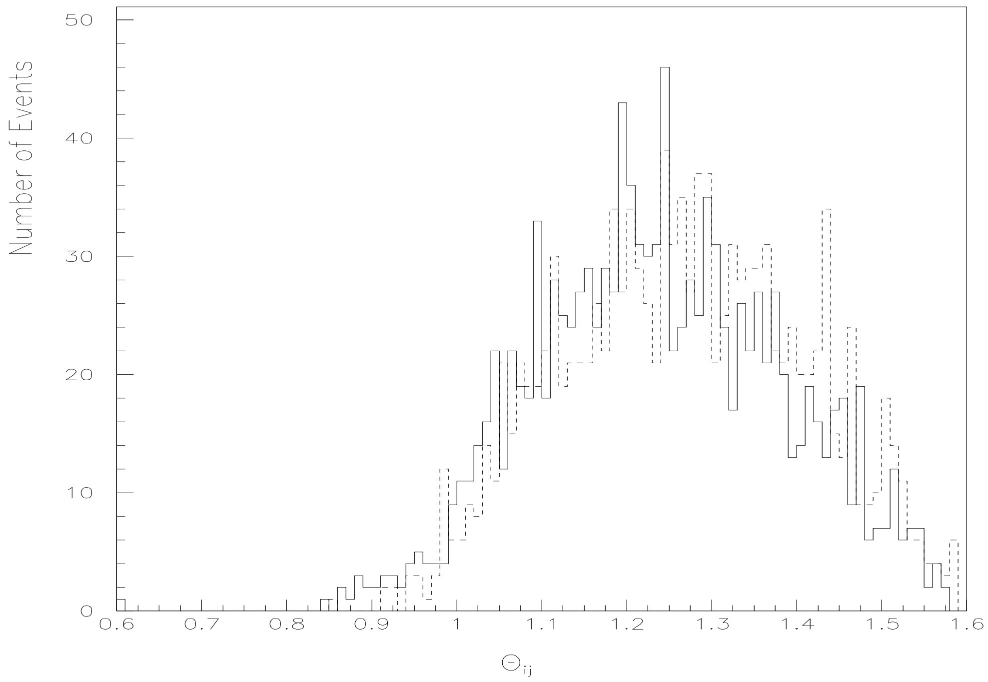

Figure 12: $theta_{ij}$ distributions for the events from the decay chamber (upper plot) and the events from the umbilic (bottom plot), solid line are real data while dashed distributions are produced by Monte Carlo.

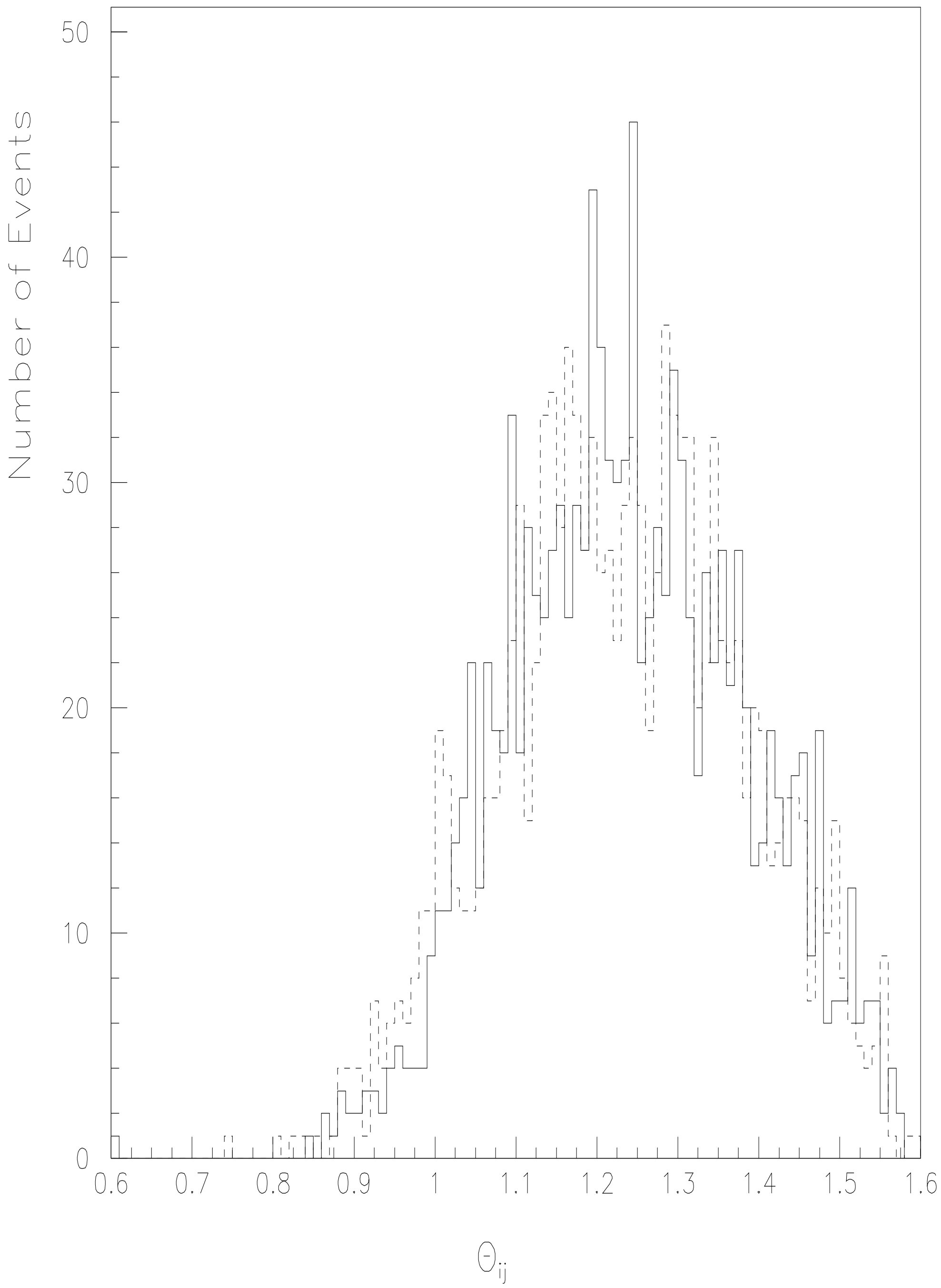

Figure 13: $theta_{ij}$ distributions for the events from the umbilic events, solid line are the data from run3597 while dashed line are the data from run4514. Run3597 is a ^{16}N run with the source located at the center of the detector while the source position in run4514 is z=-440cm. For data from run3597, a fiducial cut ($\sqrt{x_{fit}^2 + y_{fit}^2} < 200cm$ and $200cm < z_{fit} < 400cm$) was imposed while a different fiducial cut $\sqrt{x_{fit}^2 + y_{fit}^2} < 200cm$ and $-100cm < z_{fit} < 100cm$) was imposed for the data from run4514.